

Nanoelectromechanics of superconducting weak links

(Review Article)

A.V. Parafilo¹, I.V. Krive^{1,2,3}, R.I. Shekhter², and M. Jonson^{2,4,5}

¹*B. Verkin Institute for Low Temperature Physics and Engineering of the National Academy of Sciences of Ukraine
47 Lenin Ave., Kharkov 61103, Ukraine*

E-mail: parafilo_sand@mail.ru

²*Department of Physics, University of Gothenburg, SE-412 96 Göteborg, Sweden*

³*Physical Department, V.N. Karazin National University, Kharkov 61077, Ukraine*

⁴*SUPA, Department of Physics, Heriot-Watt University, Edinburgh EH14 4AS, Scotland, UK*

⁵*Department of Physics, Division of Quantum Phases and Devices, Konkuk University, Seoul 143-701, Korea*

Received December 23, 2011

Nanoelectromechanical effects in superconducting weak links are considered. Three different superconducting devices are studied: (i) a single-Cooper-pair transistor, (ii) a transparent SNS junction, and (iii) a single-level quantum dot coupled to superconducting electrodes. The electromechanical coupling is due to electrostatic or magnetomotive forces acting on a movable part of the device. It is demonstrated that depending on the frequency of mechanical vibrations the electromechanical coupling could either suppress or enhance the Josephson current. Nonequilibrium effects associated with cooling of the vibrational subsystem or pumping energy into it at low bias voltages are discussed.

PACS: **85.85.+j** Micro- and nano-electromechanical systems (MEMS/NEMS) and devices;
73.23.-b Electronic transport in mesoscopic systems;
74.50.+r Tunneling phenomena; Josephson effects;
74.45.+c Proximity effects; Andreev reflection; SN and SNS junctions.

Keywords: nanoelectromechanics, single-Cooper-pair box, short SNS junction, quantum dot.

Contents

1. Introduction.....	348
2. Single-cooper-pair box and mechanically mediated Josephson currents.....	349
3. Short vibrating SNS junctions: supercurrent and cooling of the mechanical subsystem.....	353
4. Polaronic effects in resonant Josephson current through a vibrating quantum dot.....	355
5. Conclusion.....	357
References.....	358

1. Introduction

The Josephson effect [1] is one of the most spectacular phenomena in quantum physics. Two fundamental quantum phenomena — macroscopic quantum coherence and electron tunneling — determines the Josephson coupling of separated superconductors. The theoretical prediction and experimental observation [2] of the Josephson effect gave birth to a new science — the superconductivity of weak links.

In the last decade one has seen a rapid progress in the formation and development of nanoelectromechanical systems (NEMS) which can be used as single-molecule mass

sensors, as the basic elements of nanoelectronics (single electron transistor, relay, etc.) and as effective transducers and signal processors. Recently, suspended carbon nanotube-based NEMS, which have been shown to have extraordinary electrical and mechanical properties (see, e.g., [3]), have attracted special interest.

Theory predicts a number of new effects in NEMS that are due to the interplay of their electronic and vibrational subsystems. Among the theoretically predicted phenomena electron shuttling [4,5], phonon assisted single-electron tunneling [6,7] and the Franck–Condon (“polaronic”) blockade [8] have already been observed in experiments [9,10].

Single-wall carbon nanotubes have already been used as weak links in superconducting devices [11] and there is no doubt that transport properties of superconducting NEMS will soon be measured. Therefore it is interesting and significant to sum up our knowledge of this subject. This is the aim of the present review.

We have considered three different types of superconducting NEMS: (i) a vibrating single-Cooper-pair box coupled to superconducting electrodes, (ii) a transparent (ballistic) SNS junction with a vibrating normal part (nanotube) of the device, and (iii) a vibrating single-level quantum dot coupled by tunneling to superconducting banks. Without the adjective “vibrating”, all these devices are familiar systems in the field of superconductivity. The electromechanical coupling gives them new and unusual features. In particular, a single-Cooper-pair box could play the role of a mediator of the Josephson coupling between remote superconductors. The voltage-driven Andreev states in a transparent short SNS junction serve as the refrigerant responsible for pumping energy from the nanotube vibrations to the thermostat of quasiparticle states in the leads. A single-level vibrating quantum dot coupled to superconducting leads, depending on the vibration frequency, could either suppress the supercurrent (“hard” vibrons: $\hbar\omega_0 \gg \Delta$, Δ is the superconducting gap) or even to enhance the Josephson current if the vibrational subsystem is “soft” ($\omega_0 \rightarrow 0$) and it is ready to transform to a new ground state.

As far as we know the present paper is the first review of the nanoelectromechanics of weak links. We considered the influence of vibrations on the dc Josephson current at zero or small bias voltages (adiabatic regime). The review consist of an introduction, three sections and a conclusion. In Sec. 2 we discuss the papers on mechanically mediated Josephson currents. In Sec. 3 the supercurrent and cooling effects in a vibrating nanotube in a magnetic field are considered. In Sec. 4 we study the influence of vibrations on the resonant Josephson current in a superconductor–quantum dot–superconductor tunnel junction.

2. Single-cooper-pair box and mechanically mediated Josephson currents

The single-Cooper-pair box (SCPB) is a mesoscopic device in which a small superconducting grain is coupled by tunneling to a massive superconducting electrode via Josephson junction and is capacitively connected to a gate electrode. The Hamiltonian of the Cooper-pair box reads [12]

$$H = E_C(n - n_G)^2 - E_J \cos \varphi, \quad (1)$$

where $E_C = (2e)^2 / 2C$ is the charging energy (C is the grain capacity), $E_J = (\hbar^2 / 2e)I_c$ (I_c is the critical current) is the Josephson energy and $n_G = V_G C / 2e$ (V_G is the gate potential). The first term in Eq. (1) represents kinetic (electrostatic) energy, the second term is the potential

(Josephson) energy. In a quantum mechanical treatment the canonically conjugate variables $\varphi(t)$ and $n(t)$ obey the commutation relation $[\hat{\varphi}, \hat{n}] = 1$.

The single-Cooper-pair box is realized in the Coulomb blockade regime [13] (see also [14]),

$$\Delta \gg E_C \gg E_J; \quad T \ll E_C \quad (2)$$

(2Δ is the superconducting gap) (and it is assumed that junction resistance $R \gg R_0 = h / e^2$), where the single electron states are energetically unfavorable due to the parity effect (see, e.g., [15,16]) and the superconducting properties of the grain are described by a two-level quantum system (qubit) with (2×2) matrix Hamiltonian (see, e.g., the review [17])

$$H_{SCPB} = -\frac{1}{2}(\varepsilon\sigma_z + E_J\sigma_x). \quad (3)$$

Here $\varepsilon = E_C(1 - n_G)$, $0 \leq n_G \leq 1$ and σ are Pauli matrices. The eigenenergies of the Hamiltonian (3)

$$E_{\pm} = \pm \frac{1}{2} \sqrt{E_C^2(1 - 2n_G)^2 + E_J^2} \quad (4)$$

are controlled by the gate voltage V_G and at special values of V_G , when Coulomb blockade is lifted ($n_G = 1/2$ on modulus 1), the level splitting $\Delta E = E_J \ll \Delta$ is small and the levels are well separated from the single electron (hole) excitations.

The state vector of a SCPB is a coherent superposition of the states with $n=0$ and $n=1$ Cooper pairs on the grain, $|\psi_{SCPB}\rangle = \alpha|0\rangle + \beta|1\rangle$ ($|\alpha|^2 + |\beta|^2 = 1$). Notice that for a closed system any superposition of states with different electric charges is forbidden by the charge conservation law (superselection rules). It means that actually the SCPB state is entangled with the states of the lead $|\tilde{\psi}_{SCPB}\rangle = \tilde{\alpha}|0\rangle|\psi_{\text{lead}}\rangle + \tilde{\beta}|1\rangle|\psi'_{\text{lead}}\rangle$. When the lead is nonsuperconducting this entanglement results in decoherence of the qubit. For a superconducting lead one has to distinguish between states with a fixed number of Cooper pairs $|N\rangle$ (strong fluctuations of the superconducting phase) and states with a fixed superconducting phase $|\varphi\rangle$ (strong fluctuations of the number of Cooper pairs). In the first case $|\psi_{\text{lead}}\rangle = |N\rangle$, $|\psi'_{\text{lead}}\rangle = |N-1\rangle$ and the qubit is characterized by a diagonal density matrix (mixed state)

$$\hat{\rho}_{SCPB} = \text{Tr}_{\text{lead}} |\tilde{\psi}_{SCPB}\rangle\langle\tilde{\psi}_{SCPB}| = p_0|0\rangle\langle 0| + p_1|1\rangle\langle 1|. \quad (5)$$

The only possibility to create a coherent Josephson hybrid $|\psi_{SCPB}\rangle$ on the grain is to “entangle” the neutral $|0\rangle$ and the charged $|1\rangle$ states with a coherent state of the bulk superconductor characterized by a fixed superconducting phase $|\varphi\rangle$. In this case the number of Cooper pairs in the lead fluctuates strongly ($|\psi_{\text{lead}}\rangle = |\psi'_{\text{lead}}\rangle = |\varphi\rangle$) and the Josephson coupling of the superconducting grain with the bulk superconductor creates, in the Coulomb blockade

regime defined by Eq. (2), the factorized state $|\Psi_{SCPB}\rangle \otimes |\varphi\rangle$.

The SCPB Hamiltonian is readily generalized to the case when the superconducting grain is coupled by tunneling to two superconducting electrodes with fixed phases $\pm\varphi/2$. Such a system is called a superconducting single-electron transistor (SSET) and is described by the Hamiltonian

$$H_{SSET} = E_C(\hat{n} - n_G)^2 - E_J^L \cos(\varphi/2 - \hat{\phi}) - E_J^R \cos(\varphi/2 + \hat{\phi}). \quad (6)$$

For a symmetric junction $E_J^L = E_J^R = E_J$ the potential energy in Eq. (6) is reduced to $-2E_J \cos(\varphi/2) \cos(\hat{\phi})$ and the SSET can be described by the qubit Hamiltonian (3) provided the Josephson energy E_J is replaced by $2E_J \cos(\varphi/2)$ (φ is the superconducting phase difference).

When the Coulomb blockade is lifted ($n_G = 1/2$) the SSET eigenenergies are $E_{\pm} = \mp E_J \cos(\varphi/2)$ and the corresponding eigenstates $|\pm\rangle = (|0\rangle + |1\rangle)/\sqrt{2}$ can (when occupied) carry the partial supercurrents $J_{\pm} = (2e/\hbar)\partial E_{\pm}/\partial\varphi = \pm(eE_J/\hbar) \sin(\varphi/2)$. The average Josephson current through a SSET takes the form

$$J = \frac{2e}{\hbar} \frac{\partial \Omega}{\partial \varphi}, \quad \Omega = -T \sum_{j=\pm} \ln\left(1 + e^{-E_j/T}\right), \quad (7)$$

where Ω is the grand canonical potential. In equilibrium at given temperature T and phase difference φ one finds

$$J = \frac{eE_J}{\hbar} \sin(\varphi/2) \tanh\left[\frac{E_J \cos(\varphi/2)}{2T}\right]. \quad (8)$$

This formula coincides with the expression for the resonant Josephson current ([18,19], see also Sec. 4) through a single-level quantum dot after the replacement $E_J \rightarrow \Gamma$ ($\Gamma \ll \Delta$, Γ is the level width). Therefore Eq. (8) could be interpreted as resonant (“macroscopic”) tunneling of Cooper pairs through the charge hybrid states $|\pm\rangle$ on the grain. Correspondingly the critical current is determined by the first power of the Josephson energy E_J (and not $E_J^R E_J^L \propto E_J^2$) and the dependence on the phase φ is different from the standard Josephson relation for nonresonant electron tunneling $J \sim E_J^L E_J^R \sin\varphi$.

A single-Cooper-pair box and qubit based on SCPB were first experimentally realized [20,21]. Later, in the experiment by Nakamura et al. [22], two additional normal-metal probe electrodes (a voltage-biased electrode and a pulse-gate electrode) were attached to the superconducting island. This allows one to control the quantum states of the superconductor-based two-level system. In particular by applying a gate voltage pulse, coherent oscillations between two charge states (Rabi oscillations) were observed [22].

A movable single-Cooper-pair box can be used for the transportation of Cooper pairs. In the closed superconduct-

ing circuit shuttling of Cooper pairs results in a mechanically mediated Josephson current [23]. Even for disconnected superconducting leads, when initially the superconductors were in the states with fixed number of Cooper pairs, Cooper pair shuttling creates long distance phase coherence [24] and induces a Josephson current through the system.

What are the requirements one has to fulfill to observe mechanically assisted Josephson current? It is evident that phase coherence has to be preserved during the transportation of the Cooper-pair box between the leads and while the SCPB interacts with the superconducting bulk electrodes. Phase coherence can be maintained if the few degrees of freedom associated with the superconducting qubit are well separated from the continuum spectrum and therefore the characteristic qubit phase coherence time is longer than the transportation time. Notice that even for a nonmobile SCPB and at low temperatures the “phase breaking time” is short due to the interaction of the superconducting qubit with the environment.

As in the case of a stationary SCPB the charging energy E_C should be larger than the Josephson energy E_J and the thermal energy, see Eq. (2). This condition prevents significant charge fluctuations on the dot. Besides, the energy quantum $\hbar\omega_0$ of the mechanical vibrations has to be much smaller than all other energy scales of the problem, $\hbar\omega_0 \ll \Delta, E_C, E_J$. This assumption excludes the creation of quasiparticles and allows one to consider the mechanical transport of the SCPB as an adiabatic process.

The adiabatic shuttling of Cooper pairs between superconducting electrodes can be separated into two stages: (i) the free motion of the Cooper-pair box, and (ii) the loading and unloading of charge in the vicinity of leads. The latter processes are induced by the Josephson coupling and tunneling of Cooper pairs occur if the Coulomb blockade is lifted $E(n=0) = E(n=1)$ by the appropriate gate voltage applied near the contacts. The coherent exchange of a Cooper pair between the grain and the lead creates a “Josephson hybrid” on the grain:

$$|0\rangle \Rightarrow s_{00}|0\rangle + s_{01}e^{-i\varphi_j}|1\rangle; |1\rangle \Rightarrow s_{11}|1\rangle + s_{10}e^{i\varphi_j}|0\rangle, \quad (9)$$

where φ_j is the superconducting phase of the left ($j=L$) or right ($j=R$) electrode (we assume that the leads are in states with a given phase of the superconducting order parameter). The transition amplitudes s_{ij} are determined by the Josephson energy E_J and the time t_c spent by the grain in contact with the lead

$$|s_{00}| = |s_{11}| = \cos\theta_J, \quad |s_{01}| = |s_{10}| = \sin\theta_J, \quad \theta_J \simeq E_J t_c / \hbar. \quad (10)$$

During the free motion of the SCPB between the leads the dynamics of the qubit is reduced to the evolution of the relative phase χ of the $n=0$ and $n=1$ states $\hbar\dot{\chi} = E(n=1) - E(n=0) = E_C$. The accumulated phases

are in general different for left-to-right (t_+) and right-to-left (t_-) motion

$$\chi_{\pm} \simeq E_C t_{\pm} / \hbar. \quad (11)$$

For a periodic adiabatic motion of the SCPB with frequency $f = \omega_0 / 2\pi$ the dc Josephson current was calculated in Ref. 23. It takes the form

$$J = 2ef \frac{\sin^3 \theta_J \cos \theta_J \sin \Phi (\cos \Phi + \cos \chi)}{1 - (\cos^2 \theta_J \cos \chi - \sin^2 \theta_J \cos \Phi)^2}, \quad (12)$$

where $\Phi = \varphi_R - \varphi_L + \chi_+ - \chi_-$ and $\chi = \chi_+ + \chi_-$ is the total dynamical phase. The current Eq. (12) is an oscillating function of the superconducting phase difference $\varphi = \varphi_R - \varphi_L$, which is a direct manifestation of a Josephson coupling between the two remote superconductors.

It is useful to consider Eq. (12) in the limit of weak Josephson coupling $\theta_J \ll 1$ and vanishingly small ($t_{\pm} \rightarrow 0$) dynamical phase $\chi \rightarrow 0$. In this case Eq. (12) is reduced to the standard Josephson relation $J = J_c \sin \Phi$, where $J_c \simeq eE_J / \hbar$. For weak coupling $\theta_J \ll 1$ but a finite dynamical phase $\chi \gg \theta_J$ the mechanically assisted Josephson current is strongly suppressed, $J \propto \theta_J^3 / \sin^2 \chi \ll \theta_J$. However, the direction of the supercurrent will be opposite to the direction of the ‘‘ordinary’’ Josephson current ($J \sim \sin \Phi$) if $\cos \chi + \cos \Phi < 0$. So, for symmetric shuttling the main qualitative effect of the dynamical phase is a change of the direction of the supercurrent. In other words, for a given strength of the Josephson coupling the direction of the supercurrent is determined by the interplay of the superconducting (φ) and dynamical (χ) phases.

It is worth to stress three features, which distinguish a mechanically assisted supercurrent from the ordinary Josephson current through weak links. (1) For asymmetrical phase accumulation ($\chi_+ \neq \chi_-$) an anomalous current $J(\varphi = 0) \neq 0$ flows through the system. (2) The direction of the supercurrent at a given superconducting phase difference depends on the electrostatic phase χ . (3) The supercurrent is a nonmonotonic function of the Josephson coupling strength θ_J . The last feature is connected with the Rabi oscillations of the population of qubit quantum states induced by a switching of the Josephson interaction at the turning points of the shuttle trajectory.

Now we ask the following question: Could mechanical transportation of Cooper pairs serve as a source for the creation of phase coherence if the two superconducting leads were initially in states with a definite number of Cooper pairs? A positive answer to this question was given in Ref. 24. The entanglement of the movable Cooper-pair box with the lead states $|N_j\rangle$ ($j = L, R$) with N extra Cooper pairs results in the suppression of the relative phase fluctuations. The manifestation of this phase ordering is the appearance of an average supercurrent through the junction. Starting from an initially pure (product) state, the supercurrent

$$J = \text{Tr} \{ \hat{\rho} \hat{J} \}, \quad \hat{J} = J_c \sin (\hat{\phi}_R - \hat{\phi}_L) \quad (13)$$

($\hat{\rho}$ is the density matrix obtained by tracing the density matrix over the bath variables, $\hat{\phi}_j$ is the phase operator) was shown [24] to stabilize at a fixed value after a large number of grain rotations. The concrete number of rotations needed for current stabilization depends on the strength of the Josephson coupling. The calculated average current [24] oscillates as a function of dynamical phase χ_{\pm} similar to the previously discussed case of a mechanically assisted Josephson current. Figure 1 illustrates the behavior of the phase difference distribution as a function of the number of grain rotations. The graph shows how the system evolves (as the number of rotations increases) from a state of maximum phase fluctuations (i.e., from an initial pure charge neutral state $|\psi\rangle = |n=0\rangle |N_L=0\rangle |N_R=0\rangle$) to an entangled state

$$\sum_{n=0,1} \sum_{N_L, N_R} C_{N_L, n} \delta_{n+N_L+N_R, 0} |n\rangle |N_L\rangle |N_R\rangle \quad (14)$$

with minimum quantum fluctuations. The corresponding emergent phase difference depends on the parameters of the system and the dynamical process. It was also shown that the current is suppressed with increasing temperatures due to an increased width of the phase distribution. At low temperatures the current decays exponentially with a crossover to algebraic decay for high temperatures.

The classical mechanical motion of a simple Cooper-pair box can be modelled by letting the Josephson energy and the charging energies be time dependent. Therefore the properties of a voltage biased Josephson junction subject to an ac gate potential ($E_C(t)$) could be useful for a better

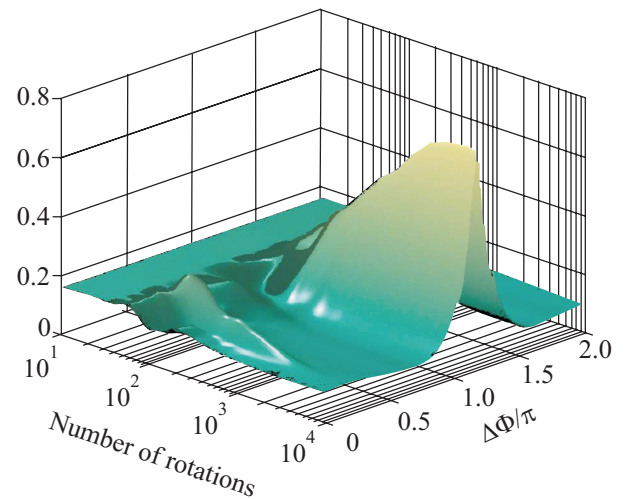


Fig. 1. Probability density for the difference $\Delta\Phi$ between the phases of the superconducting condensates of two bulk superconductors in contact via a movable superconducting grain. The grain periodically moves from one bulk superconductor to the other and the graph shows how the system evolves from a state with maximum to a state with minimum fluctuations as the number of rotation periods increases.

understanding of superconducting nanoelectromechanics. In Ref. 25 the microwave dynamics and transport properties of a voltage-biased single Cooper pair transistor were considered.

A bias voltage V makes the phase difference change with time, $\varphi(t) = \omega_J t + \varphi_0$ ($\omega_J = 2eV/\hbar$ and we set $\varphi_0 = -\pi$ for definiteness in what follows). This time dependence generates a periodic variation of the relative position of the qubit levels E_{\pm} , Eq. (4), as well as a periodic change in the partial currents J_{\pm} . The total Josephson current depends on the relative “population” δp of the levels which for a finite bias ($\omega_J \neq 0$) cross each other at times $t_n \omega_J = 2\pi n$. Consequently δp is controlled now only by relaxation processes. Weak relaxation $\nu \ll \omega_J$ results in equalization of the level population and hence the Josephson current $J \propto \delta p \propto \nu$. In the limit $\nu \rightarrow 0$ not only the dc but also the ac current through the considered weak link vanishes. A time dependent gate voltage $n_G(t) \propto \cos(\omega t + \chi)$ may significantly affect the current by inducing resonant interlevel transitions and thereby changing their populations.

This situation was considered in [25] where the interlevel transitions at resonance condition $\hbar\omega = 2E_J \sin(\omega_J t_r/2)$ were used for current stimulation. Landau–Zener interlevel transitions occur, and the level populations are changed, during the short time interval δt_r near the times $t_r^{(n)}$. Between these “scattering events” the system is in “free motion” and the level populations are “frozen”. The two different frequencies $\Omega = \omega_J/2$ and ω , which determine the ac properties of the superconducting qubit, make the dynamics of this two-level system highly nontrivial. If the ratio ω/Ω is an irrational number the dynamics is quasi-periodic and the dc Josephson current is still zero even under microwave irradiation. When $\omega/\Omega = N + p/q$ (where N and $p < q$ are integers) a finite dc supercurrent flows through the system even in the limit of weak dissipation $\nu \rightarrow 0$.

To obtain an analytical result one has to evaluate the dc Josephson current, which in our case is given by the expression

$$J = \frac{1}{T_q} \int_0^{T_q} dt \text{Tr} \{ \hat{\rho}(t) \hat{J}(t) \}, \quad \hat{J}(t) = \frac{eE_J}{\hbar} \sigma_z \cos \Omega t, \quad (15)$$

where $T_q = qT_0 = q2\pi/\Omega$, $\hat{\rho}(t)$ is a density matrix obeying the Bloch equation

$$i\hbar \frac{\partial \hat{\rho}}{\partial t} = [H(t), \hat{\rho}] - i\hbar \nu (\hat{\rho} - \hat{\rho}_0) \quad (16)$$

and $H(t)$ is the Hamiltonian of the two-level system,

$$H(t) = \sigma_z E_J \sin(\Omega t) + \sigma_x \varepsilon \cos(\omega t + \chi_0). \quad (17)$$

Here $\varepsilon/\hbar \ll \omega$ is the rate of the microwave-induced interlevel transitions and $\hat{\rho}_0(t)$ is the quasistatic density matrix

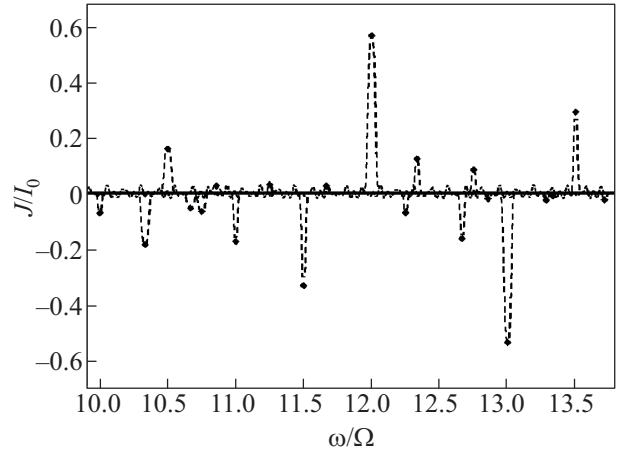


Fig. 2. Microwave-induced current J in units of $I_0 = e\omega/\pi^2$, plotted as a function the microwave frequency ω normalized to $\Omega = \omega_J/2$. The result was obtained with $\chi_0 = \pi/11$, $\hbar\omega/2E_J = 0.001$, $w = 0.5$ and $q_{\max} = 7$.

of the unperturbed ($\varepsilon = 0$) Hamiltonian (17), and ν is the relaxation rate.

The problem can be analytically solved in the weak dissipation limit. The microwave-induced dc current takes the form [25]

$$J = \frac{e\omega}{\pi^2} \arccos \left(\frac{\hbar\omega}{2E_J} \right) \frac{\tau^{2q} \tan \theta \sin(2q\chi_0)}{1 - \tau^{2q} \cos^2(q\chi_0)}, \quad (18)$$

where $\tau(\varepsilon) = 2w(\varepsilon)\sqrt{1-w(\varepsilon)} \cos \theta$ is the probability of interlevel transition ($\sqrt{w(\varepsilon)}$ is the probability amplitude of the standard Landau–Zener scattering matrix [26]) and

$$\theta = \frac{E_J}{\hbar} \int_{t_0}^{T_0/2-t_0} dt \sin \Omega t - \omega(T_0/4 - t_0), \quad (19)$$

$$t_0 = \Omega^{-1} \arcsin \frac{\hbar\omega}{2E_J}.$$

This current plotted as a function of $\omega/\Omega = \hbar\omega/eV$ demonstrates many sharp features at rational values of $\hbar\omega/eV$. The smooth dependence $J = f(\omega/\Omega)$ obtained by an interpolation procedure is shown in Fig. 2. The sharp peaks in the I – V characteristics of the microwave irradiated single Cooper pair transistor at “fractional” values of the bias voltage, $eV = \hbar\omega/(N + p/q)$, are a signature of quantum interference effects caused by the resonant interaction of the SSET with the microwave field. These peaks are finite when $N \rightarrow \infty$ and do not vanish in the limit of weak microwave irradiation $\tau \ll 1$. The calculated I – V characteristics differ qualitatively from the Shapiro effect (manifested as voltage steps in the I – V characteristics of a voltage-biased Josephson junction in an ac field, see, e.g., [25]) in classical Josephson junctions.

3. Short vibrating SNS junctions: supercurrent and cooling of the mechanical subsystem

In this section we consider the nanoelectromechanical properties of a suspended single-wall metallic carbon nanotube coupled to superconducting electrodes. Depending on the coupling strength this system can be modelled as a vibrating quantum dot (weak coupling) or SNS junction (strong coupling). The interaction of electronic and mechanical degrees of freedom in this device can be mediated either by electrical charges or currents. The electrical forces are most pronounced in the weak coupling (tunneling) regime when the number of particles on the dot is a well-defined quantity. This case will be analyzed in detail in the next section. Here we consider electromechanical effects induced by the interaction of a supercurrent with nanotube vibrations in a magnetic field.

We will model the S/SWNT/S junction as a short SNS junction (the length L of the suspended nanotube is assumed to be much shorter than the superconducting coherence length, $L \ll \xi_0 \simeq \hbar v_F / \Delta$). It is well known (see, e.g., [19,27,28]) that in a one-dimensional (single channel) short SNS junction the spectrum of Andreev bound states is reduced to two states with energies $E_{\pm}(\varphi) = \pm E_A(\varphi)$, $E_A(\varphi) = \Delta[1 - D \sin^2(\varphi/2)]^{1/2}$, where $0 \leq D \leq 1$ is the junction transparency. When occupied these levels carry supercurrents in opposite directions. The equilibrium Josephson current at temperature T reads

$$J = \frac{e\Delta}{2\hbar} \frac{D \sin \varphi}{\sqrt{1 - D^2 \sin^2(\varphi/2)}} \tanh\left(\frac{E_A}{2T}\right). \quad (20)$$

The supercurrent produced by the continuum spectrum (scattering states) is zero in the considered limit $L/\xi_0 \rightarrow 0$. Since the continuum spectrum does not contribute to the current the Hamiltonian of a short SNS junction can in many cases be represented by the Hamiltonian of a two-level system (Andreev qubit [29,30])

$$H_A = \sigma_z \Delta \cos(\varphi/2) + \sigma_x \Delta \sqrt{R} \sin(\varphi/2), \quad (21)$$

where $R = 1 - D$ is the reflection coefficient. The supercurrent operator is defined as $\hat{J} = (2e/\hbar)(\partial E_A / \partial \varphi) \sigma_z$ and in equilibrium it results in the average Josephson current Eq. (20). The qubit Hamiltonian Eq. (21) is readily diagonalized by the unitary transformation

$$\begin{aligned} \tilde{H}_A &= U^\dagger H_A U = E_A(\varphi) \sigma_z, \quad U = \exp(-i\theta \sigma_y), \\ \tan 2\theta &= \sqrt{R} \tan(\varphi/2). \end{aligned} \quad (22)$$

In the basis of Andreev levels the current operator takes the form

$$\hat{J} = \frac{2e}{\hbar} \frac{\partial E_A}{\partial \varphi} (\sigma_z \cos 2\theta - \sigma_x \sin 2\theta). \quad (23)$$

Although the Hamiltonian (21) is formally valid for all values of the reflection coefficient in the interval $0 \leq R \leq 1$

it is ‘‘in practice’’ used as a qubit Hamiltonian only for transparent junctions with $R \ll 1$. In this limit the energy gap (at $\varphi \approx \pi$) between Andreev states is small, $\delta E_g = 2\Delta\sqrt{R} \ll \Delta$, and the energy levels are well separated from the continuum states, which introduce dissipation in the dynamics of the Andreev qubit.

The electromechanical coupling in our system is phenomenologically introduced by applying a magnetic field H perpendicular to the direction of the current. It is assumed that the magnetic field acts only on the normal part of the SNS junction. Then the nanotube is deflected due to the Laplace force $F = (1/c)L\hat{J}\mathcal{H}$. The corresponding interaction term $H_{\text{int}} = \hat{F}y$ represents the coupling of electrical and mechanical degrees of freedom. Vibrations of the nanotube are modelled by a harmonic potential and the total Hamiltonian reads

$$H = H_A + 2\alpha_{\mathcal{H}} \frac{dE_A}{d\varphi} (b^\dagger + b)\sigma_z + \hbar\omega_0 b^\dagger b, \quad (24)$$

where b^\dagger (b) is the creation (destruction) operator of a vibrational mode with frequency ω_0 , $\Phi_0 = hc/e$ is the flux quantum, $\alpha_{\mathcal{H}} = 2\pi\Phi_{\mathcal{H}}/\Phi_0$ is the dimensionless strength of electron–vibron interaction ($\Phi_{\mathcal{H}} = \mathcal{H}Ll_0$, $l_0 = \sqrt{\hbar/2m\omega_0}$ is the amplitude of zero-point vibrations).

Notice that the electron–vibron coupling results in an effective electron–electron interaction and hence the concept of Andreev qubit Eq. (21) (derived for noninteracting electrons) is not valid in the general case. Besides, the interaction term is L -independent while the level energies in Eq. (21) were obtained in the limit $L \rightarrow 0$. Therefore one can justify Eq. (24) only in perturbation theory with respect to the small parameter $\alpha_{\mathcal{H}}$ and we neglect the influence of the magnetic field on the level energies. Then the current \hat{J} can be expressed in terms of the unperturbed energies of the Andreev levels. When additionally the SNS junction is transparent ($R \ll 1$) the derivative of the level energies with respect to φ can be taken to be a constant, $2\delta E_A(R=0)/\delta\varphi = -\Delta \sin(\varphi/2) \simeq \Delta$ at $\varphi \approx \pi$. This model is the starting point of the considerations in Refs. 31, 32, where a new mechanism for cooling the vibrational subsystem was proposed.

The physical idea underlying the superconductivity-induced electromechanical cooling mechanism is rather simple. When a bias voltage is applied over the SNS junction the voltage-driven Andreev states play the role of a mediator responsible for pumping energy from the nanomechanical vibrations to the quasiparticle states in the leads. The ac Josephson dynamics of a short SNS junction induced by a weak dc driving voltage $eV \leq eV_c = (\delta E)^2/\Delta = 4R\Delta$ is described by an adiabatic evolution of the Andreev states. At the start of each cooling cycle the energy separation of the Andreev levels, $\delta E(\varphi) = 2E_A(\varphi)$, initially shrinks in such a way as to bring them into thermal contact (at $\varphi \simeq \pi$) with the vibrational subsystem ($\delta E_g = \hbar\omega$) and resonant energy exchange between electronic and vibronic degrees

of freedom occurs. Being thermally populated at the moment of their separation from the continuum spectrum, the Andreev states are over-cooled at $\varphi \simeq \pi$ if the thermal relaxation is not sufficiently fast to follow the level displacement. This work is done by the bias voltage. In the vicinity of the resonance point $t_r = \pi\hbar/2eV$ interlevel transitions with absorption and emission of vibronic excitations take place. It is physically evident (and justified by calculations) that scattering from the lower electronic branch (–) into the upper (+) branch with the absorption of a vibron after passing through the resonance is more probable than scattering that involves vibron emission. Analogously, inelastic transitions from the upper to the lower branch occur mostly with the emission of a vibron. This means that transitions between the over-cooled states induced by the electromechanical coupling will result in the absorption of energy from the vibronic subsystem. At the second stage ($\varphi \gtrsim \pi$) of the adiabatic evolution the absorbed energy is transferred into electronic quasiparticles when the Andreev states merge with the continuum spectrum ($\varphi \simeq 2\pi$). The process of cooling is continued through the formation of new thermally populated Andreev states and their time evolution in the next cooling cycle and so on.

A calculation of the transition rates induced by the time independent weak ($\alpha_{\mathcal{H}} \ll 1$) coupling term of the Hamiltonian (24) in the Andreev level basis $H_{\text{eff}} = E_A[\varphi(t)]\tau_3 + \alpha_{\mathcal{H}}\Delta\tau_1$ (τ_i are the Pauli matrices) yields a simple expression for the probability of inelastic scattering $|-,n\rangle \rightarrow |+,n-1\rangle$ with the absorption of a vibron (n is the number of vibrons) [32],

$$p_+(n) \simeq \pi n \Gamma^2, \quad \Gamma = \alpha_{\mathcal{H}}(\Delta/\hbar\omega_0)(V_c/V)^{2/3} \ll 1. \quad (25)$$

As the opposite process $|+,n\rangle \rightarrow |-,n+1\rangle$ is forbidden if initially only the lower branch is populated ($T \ll \Delta$), the mechanical subsystem would thus approach the vibrational ground state. Figure 3 illustrates how the probability p_n for the mechanical subsystem to have n excited quanta depends on n after $N \gg 1$ cooling cycles. Initially p_n is thermally distributed $p_n = \exp(-n\hbar\omega_0/T)[1 - \exp(-\hbar\omega_0/T)]$ and after many periods ($N \sim 10^3$) the vibrational subsystem is effectively cooled down to a small final average vibron population $\langle n \rangle \sim 0.1$.

In the end of this section we briefly discuss magnetic field-induced superconducting pumping of nanomechanical vibrations in a nanotube-based Josephson junction [33]. The interplay of elastic and superconducting properties of S/suspended nanotube/S junction is provided by a magnetic field \mathcal{H} applied perpendicular to the nanotube. Then the nanotube vibrations $u(x,t)$ are influenced by the Laplace force $F_L = (1/c)\mathcal{H}J(\varphi)L$ acting on a current-carrying tube of length L ($J(\varphi) = I_c \sin \varphi$ is the Josephson current). The dynamics of the superconducting phase difference φ , controlled by the Josephson relation $\dot{\varphi} = (2e/\hbar)V$ (V is the bias voltage), is affected by the magnetic field due to an electromotive force ($V \rightarrow V - (\mathcal{H}/c)\int dxu(x,t)$)

experienced by the wire moving in the static magnetic field. The set of nonlinear dynamical equations for the amplitude $a(t)$ of vibrations ($u(x,t) = u(x)a(t)$, where $u(x)$ is the profile of the nanotube bending mode) and the phase $\varphi(t)$ in dimensionless variables reads [33]

$$\ddot{Y} + \gamma\dot{Y} + Y = \epsilon \sin \varphi, \quad \dot{\varphi} = \tilde{V} - \dot{Y}. \quad (26)$$

Here $Y(\tilde{t}) = (4eL\mathcal{H}/\hbar)a(\tilde{t})$, $\tilde{V} = 2eV/\hbar\omega_0$ (ω_0 is the frequency of the bending mode), $\epsilon = 8eL^2\mathcal{H}^2I_c/\hbar m\omega_0^2$ and γ is the dimensionless damping coefficient which is assumed to be small. The dimensionless time \tilde{t} in Eq. (26) is measured in units of ω_0^{-1} . The dc Josephson current through the system is $j_{dc} = (\gamma/V)\langle \dot{a}^2(\tilde{t}) \rangle$, where $\langle \dots \rangle$ denotes time-averaged quantity. Numerical simulations of Eq. (26) performed in [33] when both dimensionless parameters are small ($\epsilon, \gamma \ll 1$) revealed distinct resonance peaks in the vibration amplitude at integer values of bias voltage. For small vibration amplitudes there is a resemblance between the considered resonances in the Josephson junction coupled to elastic vibrations and the Fiske effect (see, e.g., [34]) in Josephson junctions coupled to an electromagnetic resonator. In particular $\tilde{V} = 1$ corresponds to a direct resonance and $\tilde{V} = 2$ represents a parametric resonance. However, in the nonlinear regime, which holds when the driving force is large $\epsilon > \gamma$, the resonances in the considered system are significantly different from those of the Fiske effect. It was shown [33] that for realistic experimental parameters the system can be driven into a multistable regime by varying the strength of magnetic field. The ac Josephson current on resonance initially grows with increasing magnetic field, but then falls off as $1/\mathcal{H}^2$ as the vibration amplitude is saturated. The predicted in [33] mul-

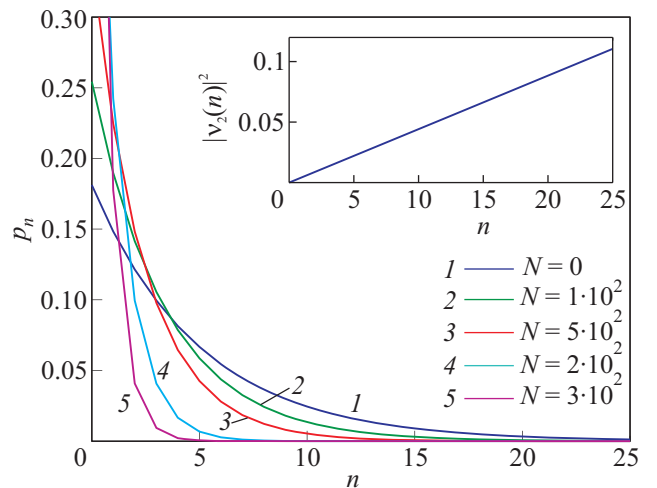


Fig. 3. (Color online). Evolution of the distribution of the mechanical modes, p_n , as a function of the quantum state n for different number of periods N ($T_V = \pi\hbar/eV \sim 20$ ns). Initially, p_n is thermally distributed, $p_n \propto \exp(-n\hbar\omega_0/T)$, with $T = 5\hbar\omega_0$. Here $\hbar\omega_0 = 10^{-6}$ eV, $\Delta = 10\hbar\omega_0$, $l_0 = 20$ pm, $L = 100$ nm, $\mathcal{H} = 1$ T. The inset shows the probability amplitude for the system to scatter out of the initial Andreev state as a function of n for the same parameters.

tistability of nanotube vibrations could result in hysteresis-like behavior of dc Josephson current as a function of bias voltage.

4. Polaronic effects in resonant Josephson current through a vibrating quantum dot

In this section we consider the influence of a strong electron–vibron interaction on the Josephson current. Recently experiments with suspended carbon nanotubes revealed a remarkably large electron–vibron coupling in normal electron transport through nanotube-based quantum dots [10,35–37]. In the cited transport experiments the vibrational effects were observed in the regime of Coulomb blockade and the electromechanical coupling was induced by the interaction of an extra charge on the vibrating tube with the gate potential. Carbon nanotube-based junctions have already been used in tunneling superconducting devices [11]. Therefore one could expect strong electromechanical effects in superconducting transport in SNS junctions with suspended nanotubes as well.

Here we consider the simplest model of a vibrating quantum dot (QD) coupled to superconducting electrodes via tunneling junctions. The dot is modelled by a single spin-degenerate ($\sigma = \uparrow, \downarrow$) level interacting with a single vibronic mode ($\hbar\omega_0$)

$$H_{QD} = \sum_{\sigma=\uparrow,\downarrow} \varepsilon_0 d_\sigma^\dagger d_\sigma + U n_\uparrow n_\downarrow + \varepsilon_i \hat{n} (b^\dagger + b) + \hbar\omega_0 b^\dagger b, \quad (27)$$

where d_σ (d_σ^\dagger) is the destruction (creation) operator for an electron on the dot with spin projection $\sigma = \uparrow, \downarrow$ and energy ε_0 measured from the Fermi level, $\hat{n}_\sigma = d_\sigma^\dagger d_\sigma$, $\hat{n} = \hat{n}_\uparrow + \hat{n}_\downarrow$, b (b^\dagger) is the vibronic destruction (creation) operator, U is the energy of electron–electron interaction and ε_i is the energy of electron–vibron interaction. Using this model is a standard approach to studying vibrational effects in single-molecule transistors (see, e.g., the reviews [38,39]). In Ref. 40 this Hamiltonian was used for studying the effects of electron–vibron interactions on the Josephson current through superconductor–QD–superconductor (S/QD/S) junction (see, e.g., [41]). The left ($j = L$) and right ($j = R$) superconducting electrodes are described by the standard BCS Hamiltonian

$$H_j = \sum_{k,\sigma=\uparrow,\downarrow} \varepsilon_{k,j} c_{k\sigma j}^\dagger c_{k\sigma j} - \left(\sum_k \Delta_j c_{k j \uparrow}^\dagger c_{-k j \downarrow}^\dagger + \text{h.c.} \right) \quad (28)$$

($\Delta_j = |\Delta| e^{i\phi_j}$ is the superconducting order parameter), and the QD–S coupling is described by the tunneling Hamiltonian

$$H_{tj} = \sum_{k,\sigma=\uparrow,\downarrow} t_{kj} c_{k\sigma j}^\dagger d_\sigma + \text{h.c.} \quad (29)$$

The standard trick used in treating the Hamiltonian (27) (see, e.g., [42]) is to eliminate the electron–vibron interaction by the unitary transformation $U = \exp(i\lambda \hat{p} \hat{n})$

($\hat{p} = i(b^\dagger - b)/\sqrt{2}$ is the dimensionless momentum operator, $\lambda = -\sqrt{2}\varepsilon_i / \hbar\omega_0$ is the dimensionless electron–vibron interaction strength). The transformation results in a (polaronic) shift of the dot level, $\varepsilon_p = \varepsilon_0 - \lambda^2 \hbar\omega_0$, and the Coulomb interaction energy, $U_p = U - 2\lambda^2 \hbar\omega_0$, in the QD Hamiltonian. The electron–vibron interaction reappears in the transformed tunneling Hamiltonian via the replacement $t_{kj} \Rightarrow t_{kj} e^{i\lambda \hat{p}}$ in Eq. (29). The average current $J = J_L = -J_R$ is represented as the thermal average of the tunneling Hamiltonian

$$J_j = i(e/\hbar) \langle [H, \hat{N}_j] \rangle = 2(e/\hbar) \text{Im} \sum_{k\sigma} \langle t_{kj}^* d_\sigma^\dagger c_{k\sigma j} \rangle, \quad (30)$$

where H is the total Hamiltonian, \hat{N}_j is the number operator for electrons on the left or right electrode and the average $\langle \dots \rangle$ is taken with the total Hamiltonian. In perturbation theory with respect to the tunneling Hamiltonian the averages of fermionic (electrons) and bosonic (vibrons) operators factorize and can be evaluated analytically in limiting cases (see below). The critical Josephson current $J(\varphi) = I_c \sin \varphi$ (φ is the superconducting phase difference $\varphi = \varphi_R - \varphi_L$) reads [40]

$$I_c = -\frac{e\Gamma_L \Gamma_R \Delta^2}{\hbar\pi^2} \int_0^\beta d\tau_1 \int_0^\beta d\tau_2 \int_0^\beta d\tau_3 \mathbf{H}(\tau_1 - \tau_2) \times \mathbf{H}(\tau_3) \mathbf{F}(\tau_1, \tau_2, \tau_3) \mathbf{B}(\tau_1, \tau_2, \tau_3), \quad (31)$$

where $\beta = 1/T$, $\mathbf{H}(\tau) = K_0(|\tau\Delta|) - K_0((\beta - |\tau|)\Delta)$ ($K_0(x)$ is a modified Bessel function), $\Gamma_j = 2\pi \sum_k |t_{kj}|^2 \delta(\varepsilon - \varepsilon_{kj})$ is the partial level width, which is energy independent in the wide band approximation. The fermion and vibron correlation functions are

$$\mathbf{F}(\tau_1, \tau_2, \tau_3) = \langle T_\tau \{ d_\downarrow^\dagger(\tau_1) d_\uparrow^\dagger(\tau_2) d_\downarrow(\tau_3) d_\uparrow(0) \} \rangle, \quad (32)$$

$$\mathbf{B}(\tau_1, \tau_2, \tau_3) = \langle T_\tau \{ e^{-i\lambda \hat{p}(\tau_1)} e^{-i\lambda \hat{p}(\tau_2)} e^{i\lambda \hat{p}(\tau_3)} e^{i\lambda \hat{p}} \} \rangle,$$

where now the averages are taken with the transformed QD Hamiltonian (which is a quadratic in the vibron operators). In the absence of electron–vibron ($\lambda = 0$) and Coulomb ($U = 0$) interactions an evaluation of the integrals in Eq. (31) for $|\varepsilon_0| \lesssim T \ll \Delta$ and $\varepsilon_0 \ll \Delta$ results in the simple expression (see, e.g., [43])

$$I_c = \frac{e}{\hbar} \frac{\Gamma^2}{2\varepsilon_0} \tanh\left(\frac{\varepsilon_0}{2T}\right). \quad (33)$$

The perturbative result (33) does not describe the resonant transport $\varepsilon_0 \rightarrow 0$, $T \rightarrow 0$. For noninteracting electrons a nonperturbative (in Γ) analysis of Eq. (31) predicts a saturation of the critical resonant ($\varepsilon_0 = 0$) current $I_c \simeq e\Gamma/\hbar$ at $T \rightarrow 0$. The resonant supercurrent through a single-level noninteracting QD can be calculated by using the spectrum of Andreev levels in a short SINIS (“I” stands for insulating barrier) with strong barriers at the NS boundaries (see, e.g., [18,19,41]). In our notation the spectrum of bound

states is $E_A(\varphi) = \pm\sqrt{\varepsilon_0^2 + \Gamma^2 \cos^2(\varphi/2)}$ and the corresponding Josephson current reads

$$J(\varphi) = \frac{e}{2\hbar} \frac{\Gamma^2 \sin \varphi}{\sqrt{\varepsilon_0^2 + \Gamma^2 \cos^2 \varphi/2}} \tanh \left(\frac{\sqrt{\varepsilon_0^2 + \Gamma^2 \cos^2 \varphi/2}}{2T} \right). \quad (34)$$

In the perturbative region ($\Gamma \rightarrow 0$) Eq. (34) reproduces the critical current Eq. (33). For resonant transport ($\varepsilon_0 = 0$) the Josephson current $J_r = (e\Gamma/2\hbar)(\sin \varphi/|\cos(\varphi/2)|)$ is strongly enhanced.

A finite Coulomb interaction, $U \neq 0$, tends to suppress the Josephson current by splitting the dot level. If $U \gg \Gamma$ the conditions for resonant tunneling can not be satisfied and the critical current $I_c \sim \Gamma^2$. In the limit of strong Coulomb interaction $U \rightarrow \infty$ (physically $U \gg \Delta$) the critical current can be evaluated analytically. Here we consider the most interesting case, where $\Gamma, \varepsilon_0 \ll \Delta$. Then for temperatures $T \ll \Delta$ and for $|\varepsilon_0| > \Gamma$ the critical current takes the form (up to a numerical factor of order one)

$$I_c \simeq \frac{\Gamma^2 \varepsilon_0}{\Delta T}. \quad (35)$$

We see that the supercurrent direction depends on the sign of ε_0 and for $\varepsilon_0 < 0$ the considered superconducting weak link acts as a “ π ”-junction [44]. The appearance in Eq. (35) of an additional small factor $|\varepsilon_0|/\Delta \ll 1$ in comparison with the analogous noninteracting expression, Eq. (33), is explained by virtual depairing of Cooper pairs in transition through a single spin-polarized electronic level. At $T \rightarrow 0$, $\varepsilon_0 \rightarrow 0$ the critical current reads $I_c \sim (e/\hbar)(\Gamma^2/\Delta) \text{sgn}(\varepsilon_0)$. The current is strongly suppressed (by “depairing” factor $\Gamma/\Delta \ll 1$) in comparison with the resonant critical current $\sim e\Gamma/\hbar$.

The electron–vibron interaction introduces an extra energy scale, the vibron energy quantum $\hbar\omega_0$, to the problem. It is clear that one could expect maximum effect of zero-point fluctuations of dc Josephson current in the limit when superconducting transport affects only the ground state of the vibrational subsystem. In the case of strong electron–electron interaction $|U_p| \gtrsim \Delta$ the considered regime is realized when $\hbar\omega_0 \gg \Delta$. For a weak effective interaction $|U_p| \rightarrow 0$ the corresponding inequality reads $\hbar\omega_0 \gg \max\{\varepsilon_0, \Gamma\}$. The bosonic correlation function $\mathbf{B}(\tau_1, \tau_2, \tau_3)$ can be expressed as exponential of the sum of two-point correlation functions $\langle\langle \hat{p}(\tau)\hat{p} \rangle\rangle = \langle \hat{p}(\tau)\hat{p} \rangle - \langle \hat{p}^2 \rangle$ which are readily evaluated for equilibrated vibrons. At low temperatures $T \rightarrow 0$ this correlation function in the considered high-frequency limit does not depend on τ and $\mathbf{B} \simeq \exp(-2\lambda^2)$. This current suppression is known as the Franck–Condon (polaronic) blockade of low-temperature and low-voltage electron transport [8,38]. The additional factor 2 in the exponent, compared to the normal transport result, accounts for the correlated tunneling of two electrons. In other words the Josephson current through a vi-

brating QD is strongly suppressed at low temperatures due to a polaronic narrowing of the level width, $\Gamma \Rightarrow \Gamma_\lambda = \Gamma \exp(-\lambda^2)$. Contrary to the normal-transport case, where the considered current suppression is absent for resonant tunneling (when the conductance ceases to depend on Γ_λ) the Josephson current is suppressed by zero-point fluctuations of the vibrating QD even for resonance conditions.

This result is confirmed by a direct calculation [45] of the resonant Josephson current through a single-level vibrating quantum dot. In particular the approach used in the cited paper allows one to evaluate the resonant current for an asymmetric S–QD–S junction ($\Gamma_L \neq \Gamma_R$), which will be important for us when considering the adiabatic regime of vibrations (see below).

Since in the superconducting leads the quasiparticles have a gap Δ in their excitation spectrum, the bulk fermions can be integrated out, which leads to an effective Hamiltonian for the dot degrees of freedom. For $\Gamma, \varepsilon_0, T, \hbar\omega_0 b \ll \Delta$ and $U = 0$ the effective Hamiltonian reads [45]

$$H_{\text{eff}} = [\varepsilon_0 - \varepsilon_i(b^\dagger + b)] \sum_{\sigma=\uparrow, \downarrow} \left(\hat{n}_\sigma - \frac{1}{2} \right) + \hbar\omega_0 b^\dagger b + \Gamma_t d^\dagger (\sigma_x \cos \varphi/2 + \gamma \sigma_y \sin \varphi/2) d, \quad (36)$$

where $d^\dagger = (d_\uparrow^\dagger, d_\downarrow^\dagger)$, $\Gamma_t = \Gamma_L + \Gamma_R$ is the total level width and $\gamma = (\Gamma_L - \Gamma_R)/(\Gamma_L + \Gamma_R)$ is the asymmetry parameter. It is clear that for superconducting transport in the considered regime $\Delta \rightarrow \infty$ only two fermion states on the dot are relevant: unoccupied $|0\rangle$ and double occupied $|\uparrow\downarrow\rangle$ fermion level (in Eq. (36) the total energy was shifted so that $E_0 = -\varepsilon_0$, $E_{\uparrow\downarrow} = \varepsilon_0$). In this basis (represented by τ_j Pauli matrices) Hamiltonian Eq. (36) after rotation $\tilde{H}_{\text{eff}} = e^{-i\tau_3\chi/2} H_{\text{eff}} e^{i\tau_3\chi/2}$, $\chi = \arctan[\gamma \tan(\varphi/2)]$ takes the form of the Hamiltonian for a two-level system (qubit) interacting with harmonic oscillator

$$\tilde{H}_{\text{eff}} = -[\varepsilon_0 - \varepsilon_i(b^\dagger + b)]\tau_3 + \hbar\omega_0 b^\dagger b + \Gamma_t \tau_1 \sqrt{\cos^2 \varphi/2 + \gamma^2 \sin^2 \varphi/2}. \quad (37)$$

We analyze this model in the limit of a strongly asymmetric junction $\gamma \rightarrow \pm 1$. The opposite case of a symmetric junction ($\gamma \rightarrow 0$, $\Gamma_L = \Gamma_R = \Gamma$) results, as expected, in a resonant supercurrent with a renormalized level width $J_r = (e/\hbar)\Gamma e^{-\lambda^2} \sin(\varphi/2) \text{sgn}[\cos(\varphi/2)]$. For an asymmetric junction the Josephson current at resonance reads

$$J = \frac{e}{2\hbar} \frac{(1-\gamma^2)\Gamma_t e^{-\lambda^2} \sin \varphi}{\sqrt{\cos^2(\varphi/2) + \gamma^2 \sin^2(\varphi/2)}}. \quad (38)$$

We see that the maximum Josephson current flows in symmetric junctions and that the supercurrent in a strongly asymmetric ($\Gamma_{R(L)} \ll \Gamma_{L(R)}$, i.e. $\gamma \approx \pm 1$) junction is determined (as it should be) by the smallest transparency of

the barriers, $J_{\text{asym}} = (2e/\hbar)(\Gamma_L\Gamma_R/\Gamma_t)\exp(-\lambda^2)\sin\varphi$. In the considered limit of “hard” vibrons ($\hbar\omega_0 \gg \Gamma, \varepsilon_0$) the vibration-induced suppression of current ($\sim \exp(-\lambda^2)$) does not depend on the asymmetry parameter γ .

It is worth to mention here that a novel type of Andreev bound state spectroscopy based on a dispersive measurement of polaron states on a quantum dot strongly coupled to a bosonic subsystem (QED cavity) was suggested in Ref. 46.

In the end of this section we briefly consider the opposite (adiabatic) limit of “soft” vibrons $\hbar\omega_0 \rightarrow 0$. In this case the elastic energy associated with the vibrons is small and the vibronic subsystem can be easily excited and transformed to a new ground state ($\langle x \rangle \neq 0$) of an interacting fermion–boson system. In the adiabatic limit the fast fermionic degrees of freedom can be integrated out, resulting in an effective nonquadratic potential U_{eff} for the vibrons. When calculating the Josephson current one can distinguish two cases: (i) the level widths Γ_j do not depend on coordinate, and (ii) a shift of the oscillator-center-of-mass strongly affects the tunneling rates Γ_j/\hbar .

The last case can be realized for instance in a superconducting variant of the C_{60} -based molecular transistor [9]. Notice that for normal transport the assumption (ii) could result in electron shuttling [47]. For a dc Josephson effect energy pumping in the vibrational subsystem is impossible and, instead of shuttling, one could expect a static shift of the center-of-mass of the vibrating QD if the dot displacement will increase the supercurrent. As it was shown above the maximum resonant supercurrent flows in a symmetric ($\Gamma_L = \Gamma_R$) junction. Therefore, if initially the QD position in the gap between the superconducting electrodes corresponds to an asymmetric junction $\Gamma_{L(R)}^{(0)} \gg \Gamma_{R(L)}^{(0)}$ the S–QD–S junction will nevertheless act as perfectly symmetric junction $\Gamma_L(x = x_m) = \Gamma_R(x = x_m)$ due to a shift of the oscillator $x \rightarrow x_m$ for some values of phase difference and the energy of resonant level.

A more subtle quantum effect is the appearance of a new (shifted) quantum state of the vibrational subsystem due to quantum fluctuations of the fermion vacuum. In general, fermion loops (polarization “bubble” diagrams) contribute negatively to the ground-state energy. It means that for a sufficiently strong electron–vibron interaction the classical ground state of vibrons, $x = 0$, becomes unstable and a new minimum of the effective vibronic potential appears.

In Ref. 48 it was shown by numerical calculations that in the limit $\hbar\omega_0 \ll \Delta \ll \Gamma$ the effective potential $U_{\text{eff}}(x)$ for vibrons takes the form of an asymmetric double-well potential in a certain region of phase-difference space φ (the effective electron–vibron coupling depends on φ and becomes strong, see Ref. 48). The frequency of vibrons ω'_0 in the new (shifted) ground state is smaller than ω_0 and hence the effective dimensionless electron–vibron coupling $\lambda \sim \omega_0^{-3/2}$ is increased $\lambda' > \lambda$. Correspondingly,

the Josephson current is decreased. Naively, one would expect the appearance of sharp features in the phase dependence of the current at critical values of φ when the vibronic system is shifted to a new ground state. Numerical calculations performed in [48] for the case $\Gamma \gg \Delta$, when continuum states strongly affect the current, revealed only cusps in the $J = J(\varphi)$ dependence, which, however, could be significant for the noise properties of S–QD–S junctions.

Notice that in the regime of almost transparent junctions ($\Gamma \gg \Delta$, $\lambda \ll 1$) the electron–vibron interaction can be taken into account by a vibron-induced renormalization of the junction transparency in a SNINS junction [49]. Scattering of tunneling electrons on the zero-point fluctuations results in an effective transmission probability $T_{\text{eff}} = 1 - \lambda^2 / 8(\hbar\omega_0/\Gamma)^2$ of the SNINS junction [19,49].

5. Conclusion

It is useful to compare vibrational effects in normal metal and superconducting transport through a quantum dot. If the bare tunneling matrix elements are coordinate-independent quantities, the electron–vibron interaction tends to suppress the electrical current (both normal and superconducting) by “dressing” the tunneling electrons with vibron excitations on the dot.

For normal electron transport the vibron-induced suppression is most pronounced in the regime of sequential electron tunneling ($T \gg \Gamma$) where the peak conductance (at $\varepsilon_0(V_g) = 0$) scales as Γ_λ/T at low temperatures $T \ll \hbar\omega_0$ with a renormalized (suppressed) tunneling width $\Gamma_\lambda = e^{-\lambda^2}\Gamma_L\Gamma_R/(\Gamma_L + \Gamma_R)$. In superconducting transport we found an identical vibron-induced suppression of the resonant Josephson current in the limit of “hard” vibrons $\hbar\omega_0 \gg \Delta$. The Franck–Condon blockade (FCB) of normal transport is manifested as an enhancement of the satellite peaks and in the anomalous (nonmonotonic) temperature dependence of the conductance at $T \gtrsim \hbar\omega_0$ [50]. For the Josephson current a partial lifting of the FCB could be expected for “soft” vibrons $\Gamma \ll \hbar\omega_0 \ll \Delta$ in the temperature region $\hbar\omega_0 \lesssim T \ll \Delta$. So far this interesting problem has not been considered in the literature.

Another experimentally observed nanoelectromechanical effect in normal electron transport through quantum dots is electron shuttling. This phenomenon occurs at finite bias voltage (in ideal situation at $eV > \hbar\omega_0$) when both the electron–vibron interaction and a dependence of the tunneling matrix elements on coordinate are taken into account (see, e.g., the reviews [51,52]). Electron shuttling is a strongly nonequilibrium process when energy from the electrons (provided by the battery) is pumping into the vibrational subsystem. For equilibrium superconducting transport ($V = 0$), instead of electron shuttling one could expect the transition of “soft” vibrons $\hbar\omega_0 \rightarrow 0$ to a new ground state. The problem of Cooper pair shuttling through

a vibrating single-level quantum dot at finite bias voltages is still an open question.

Superconductivity introduces two special features to nanoelectromechanics, namely, coherence and the additional low-energy scale Δ . In our review we considered coherent effects mostly associated with the electron transport near the Fermi level. The peculiarities of vibrational effects when continuum spectrum is involved in superconducting transport (although they are partly studied in the literature, see, e.g., Refs. 48, 49), were not in the center of our considerations. Notice also, that among a number of papers on superconducting nanoelectromechanics where the vibrational subsystem is modelled by external time-dependent field (see, e.g., [53–56]) we reviewed only the first publications.

Despite the fact that our review is brief and we could not comment on all published papers in the field, we hope that the first retrospective view on the already solved problems in nanoelectromechanics of weak links will induce further interest both in theoreticians and experimentalists to this new area of physics.

Acknowledgments

We thank L. Gorelik, S. Kulinich and V. Shumeiko for valuable discussions. Financial support from the National Academy of Science of Ukraine (grant No. 4/10-H "Quantum phenomena in nanosystems and nanomaterials at low temperatures"), the Swedish VR, and the Korean WCU program funded by MEST/NFR (R31-2008-000-10057-0) is gratefully acknowledged. I.V.K. acknowledges the hospitality of the Department of Physics at the University of Gothenburg.

1. B.D. Josephson, *Phys. Lett.* **1**, 251 (1962).
2. P.W. Anderson and J.M. Rowell, *Phys. Rev. Lett.* **10**, 230 (1963); I.K. Yanson, V.M. Svistunov, and I.M. Dmitrenko, *Zh. Eksp. Teor. Fiz.* **47**, 2091 (1964) [*Sov. Phys. JETP* **20**, 1404 (1965)].
3. A. Cleland, *Foundations of Nanomechanics*, Springer (2003); M. Poot and H.S.J. van der Zant, *arXiv:1106.2060*.
4. L.Y. Gorelik, A. Isacsson, M.V. Voinova, B. Kasemo, R.I. Shekhter, and M. Jonson, *Phys. Rev. Lett.* **80**, 4526 (1998).
5. L.M. Jonson, L.Y. Gorelik, R.I. Shekhter, and M. Jonson, *Nano Lett.* **5**, 1165 (2005).
6. L.I. Glazman and R.I. Shekhter, *Zh. Eksp. Teor. Fiz.* **94**, 292 (1988) [*Sov. Phys. JETP* **67**, 163 (1988)].
7. S. Braig and K. Flensberg, *Phys. Rev.* **B68**, 205324 (2003).
8. J. Koch and F. von Oppen, *Phys. Rev. Lett.* **94**, 206804 (2005).
9. H. Park, J. Park, A.K.L. Lim, E.H. Anderson, A.P. Alivisatos, and P.L. McEuen, *Nature* **407**, 57 (2000).
10. R. Leturcq, Ch. Stampfer, K. Inderbitzin, L. Durrer, Ch. Hierold, E. Mariani, M.G. Shultz, F. von Oppen, and K. Ensslin, *Nature Physics* **5**, 327 (2009).
11. A.Yu. Kasumov, R. Deblock, M. Kociak, B. Reulet, H. Bouchiat, I.I. Khodos, Yu.B. Gorbatov, V.T. Volkov, C. Journet, and M. Burghard, *Science* **284**, 1508 (1999).
12. K.K. Likharev, *Dynamics of Josephson Junctions and Circuits*, Gordon and Breach (1986).
13. R.I. Shekhter, *Zh. Eksp. Teor. Fiz.* **63**, 1410 (1972) [*Sov. Phys. JETP* **36**, 747 (1972)]; I.O. Kulik and R.I. Shekhter, *Zh. Eksp. Teor. Fiz.* **68**, 623 (1975) [*Sov. Phys. JETP* **41**, 308 (1975)].
14. H. van Houten, C.W.J. Beenakker, and A.A.M. Staring, *Single Electron Tunneling*, H. Grabert and M.H. Devoret (eds.), Plenum Press, NY (1992).
15. K. Matveev, M. Gisselält, L.I. Glazman, M. Jonson, and R.I. Shekhter, *Phys. Rev. Lett.* **70**, 2940 (1993).
16. P. Lafarge, P. Joyez, D. Esteve, C. Urbina, and M.H. Devoret, *Nature* **365**, 422 (1993).
17. G. Wendin and V.S. Shumeiko, *Fiz. Nizk. Temp.* **33**, 957 (2007) [*Low Temp. Phys.* **33**, 724 (2007)].
18. G. Wendin and V.S. Shumeiko, *Superlattices Microstruct.* **20**, 569 (1996).
19. A.A. Golubov, M.Yu. Kupriyanov, and E. Il'ichev, *Rev. Mod. Phys.* **76**, 411 (2004).
20. V. Bouchiat, D. Vion, P. Joyez, D. Esteve, and M.H. Devoret, *Phys. Scr.* **76**, 165 (1998).
21. Y. Nakamura, Yu. Pashkin, and J.S. Tsai, *Nature* **398**, 786 (1999); *Physica* **B280**, 405 (2000).
22. Y. Nakamura, Yu.A. Pashkin, and J.S. Tsai, *Phys. Rev. Lett.* **87**, 246601 (2002).
23. L.Y. Gorelik, A. Isacsson, Y.M. Galperin, R.I. Shekhter, and M. Jonson, *Nature* **411**, 454 (2001).
24. A. Isacsson, L.Y. Gorelik, R.I. Shekhter, Y.M. Galperin, and M. Jonson, *Phys. Rev. Lett.* **89**, 277002 (2002).
25. L.Y. Gorelik, S.I. Kulinich, R.I. Shekhter, and M. Jonson, *Phys. Rev.* **B69**, 094516 (2004).
26. S.N. Shevchenko, S. Ashhab, and F. Nori, *Phys. Rept.* **492**, 1 (2010).
27. C.W.J. Beenakker and H. van Houten, *Phys. Rev. Lett.* **66**, 3056 (1991).
28. I.O. Kulik and A.N. Omelyanchuk, *Fiz. Nizk. Temp.* **3**, 945 (1977) [*Sov. J. Low Temp. Phys.* **3**, 459 (1977)].
29. A. Zazunov, V.S. Shumeiko, E.N. Bratus', J. Lantz, and G. Wendin, *Phys. Rev. Lett.* **90**, 087003 (2003).
30. A. Zazunov, V.S. Shumeiko, E.N. Bratus', J. Lantz, and G. Wendin, *Phys. Rev.* **B71**, 214505 (2005).
31. G. Sonne, M.E. Pena-Aza, L.Y. Gorelik, R.I. Shekhter, and M. Jonson, *Phys. Rev. Lett.* **104**, 226802 (2010).
32. G. Sonne, M.E. Pena-Aza, L.Y. Gorelik, R.I. Shekhter, and M. Jonson, *Fiz. Nizk. Temp.* **36**, 1128 (2010) [*Low Temp. Phys.* **36**, 902 (2010)].
33. G. Sonne, R.I. Shekhter, L.Y. Gorelik, S.I. Kulinich, and M. Jonson, *Phys. Rev.* **B78**, 144501 (2008).
34. A. Barone and G. Paterno, *Physics and Applications of the Josephson Effect*, Wiley, NY (1982), p. 235.
35. A.K. Hüttel, M. Poot, B. Witkamp, and H.S.J. van der Zant, *New J. Phys.* **10**, 095003 (2008).

36. G.A. Steele, A.K. Hüttel, B. Witkamp, M. Poot, H.B. Heerwaldt, L.P. Kouwenhoven, and H.S.J. van der Zant, *Science* **325**, 1103 (2009).
37. B. Lassange, Yu. Tarakanov, J. Kinaret, D. Garcia-Sanchez, and A. Bachtold, *Science* **325**, 1107 (2009).
38. I.V. Krive, A. Palevski, R.I. Shekhter, and M. Jonson, *Fiz. Nizk. Temp.* **36**, 155 (2010) [*Low Temp. Phys.* **36**, 119 (2010)].
39. M. Galperin, M.A. Ratner, and A. Nitzan, *J. Phys.: Condens. Matter* **19**, 103201 (2007).
40. T. Novotny, A. Rossini, and K. Flensberg, *Phys. Rev.* **B72**, 224502 (2005).
41. A. Martin-Rodero and A. Levy Yeyati, *Adv. Phys.* **60**, 899 (2011).
42. G.D. Mahan, *Many-Particle Physics*, 2nd ed., Plenum Press, NY (1990).
43. Q.-F. Sun, B.-G. Wang, J. Wang, and T.-H. Lin, *Phys. Rev.* **B61**, 4754 (2000).
44. L.I. Glazman and K.A. Matveev, *JETP Lett.* **49**, 659 (1989) [*Pis'ma Zh. Eksp. Teor. Fiz.* **49**, 570 (1989)].
45. A. Zazunov, D. Feinberg, and T. Martin, *Phys. Rev. Lett.* **97**, 196801 (2006).
46. J. Sköglberg, T. Löfwander, V.S. Shumeiko, and M. Fogelström, *Phys. Rev. Lett.* **101**, 087002 (2008).
47. D. Fedorets, L.Y. Gorelik, R.I. Shekhter, and M. Jonson, *Europhys. Lett.* **58**, 99 (2002).
48. A. Zazunov and R. Egger, *Phys. Rev.* **B81**, 104508 (2010).
49. A. Zazunov, R. Egger, C. Mora, and T. Martin, *Phys. Rev.* **B73**, 214501 (2006).
50. P. Utko, R. Ferone, I.V. Krive, R.I. Shekhter, M. Jonson, M. Monthieux, L. Noe, and J. Nygard, *Nature Com.* **1**, 37 (2010).
51. R.I. Shekhter, Yu. Galperin, L.Y. Gorelik, A. Isacsson, and M. Jonson, *J. Phys.: Condens. Matter* **15**, 441 (2003).
52. R.I. Shekhter, L.Y. Gorelik, M. Jonson, Yu.M. Galperin, and V.M. Vinokur, *J. Comput. Theor. Nanosci.* **4**, 860 (2007).
53. L.Y. Gorelik, V.S. Shumeiko, R.I. Shekhter, G. Wendin, and M. Jonson, *Phys. Rev. Lett.* **75**, 1162 (1995).
54. R. Avriller, F.S. Bergeret, and F. Pistolesi, *Phys. Rev.* **B84**, 195415 (2011).
55. J. Fransson, J.-X. Zhu, and A.V. Balatsky, *Phys. Rev. Lett.* **B101**, 067202 (2008).
56. J. Fransson, A.V. Balatsky, and J.-X. Zhu, *Phys. Rev.* **B81**, 155440 (2010).